

Article ID: 1000-7032(2021)10-1520-11

Green-yellow Emission Ce:LuAG Transparent Ceramics for High-brightness Solid-state Lighting

LIU Qiang¹, LI Wan-yuan^{1,2}, LIU Xin^{2,3}, ZHU Yu-xuan⁴,
DENG Tao-li⁵, LI Xiao-ying^{2,3}, CHEN Peng-hui^{2,3}, TIAN Feng^{2,3},
XIE Teng-fei^{2,3}, LI Shu-xing⁵, ZOU Jun⁴, LI Jiang^{2,3*}

(1. School of Material Science and Engineering, Jiangsu University, Zhenjiang 212013, China;

2. Key Laboratory of Transparent Opto-functional Inorganic Materials, Shanghai Institute of Ceramics,
Chinese Academy of Sciences, Shanghai 201899, China;

3. Center of Materials Science and Optoelectronics Engineering, University of Chinese Academy of Sciences, Beijing 100049, China;

4. School of Science, Shanghai Institute of Technology, Shanghai 201418, China;

5. College of Materials, Xiamen University, Xiamen 361005, China)

* Corresponding Author, E-mail: lijia@mail.sic.ac.cn

Abstract: A series of $(\text{Ce}_x\text{Lu}_{1-x})_3\text{Al}_5\text{O}_{12}$ (Ce:LuAG, $x = 0.0005, 0.001, 0.002, 0.003, 0.004$) transparent ceramics were prepared *via* high-temperature reactive sintering under vacuum. The in-line transmittances of these transparent ceramics are higher than 75% at 500–800 nm with a thickness of 1.0 mm. Absorption and emission properties of ceramics with different Ce^{3+} concentrations excited by 454 nm blue LED were investigated. An adjustable correlated color temperature (CCT) (5 653–7 433 K) was obtained. The as-prepared ceramics show remarkably superior thermal and luminescent properties: a low thermal quenching (7% drop at 225 °C), and a high luminous efficacy of 179 lm/W were obtained in the 0.1% Ce:LuAG ceramics (1.0 mm thick) coupled with commercial blue In-GaN LED chips, which also shows increasing emission intensity with increasing input power (up to 3.6 W). A high flux of 3 646 lm was obtained with robust Ce:LuAG ceramics irradiated with a high laser power density of 24.6 W/mm². Obviously, the fabricated transparent Ce:LuAG ceramics are quite prospective as a highly efficient and thermally robust green-yellow color converter for high-power solid-state lighting (SSL) application.

Key words: luminescence saturation; Ce:LuAG ceramics; color converter; high-brightness

CLC number: O482.31; TQ174

Document code: A

DOI: 10.37188/CJL.20210116

高亮度固态照明用黄绿光发射 Ce:LuAG 透明陶瓷

刘 强¹, 李万圆^{1,2}, 刘 欣^{2,3}, 朱雨轩⁴, 邓陶丽⁵, 李晓英^{2,3}, 陈鹏辉^{2,3},
田 丰^{2,3}, 谢腾飞^{2,3}, 李淑星⁵, 邹 军⁴, 李 江^{2,3*}

(1. 江苏大学 材料科学与工程学院, 江苏 镇江 212013;

2. 中国科学院上海硅酸盐研究所 透明光功能无机材料重点实验室, 上海 201899;

3. 中国科学院大学 材料与光电研究中心, 北京 100049;

4. 上海应用技术大学 理学院, 上海 201418; 5. 厦门大学 材料学院, 福建 厦门 361005)

摘要: 通过固相反应结合真空烧结制备了 $(\text{Ce}_x\text{Lu}_{1-x})_3\text{Al}_5\text{O}_{12}$ (Ce:LuAG, $x = 0.0005, 0.001, 0.002, 0.003$,

收稿日期: 2021-03-31; 修订日期: 2021-04-15

基金项目: 国家重点研发计划(2017YFB0310500); 国家自然科学基金(61775226); 中国科学院前沿科学重点研究计划(QYZDB-SSW-JSC022)资助项目

Supported by National Key R&D Program of China (2017YFB0310500); National Natural Science Foundation of China (61775226); Key Research Project of the Frontier Science of the Chinese Academy of Sciences (QYZDB-SSW-JSC022)

0.004)透明陶瓷。厚度为 1.0 mm 的 Ce: LuAG 陶瓷在 500 ~ 800 nm 波长范围内的直线透过率大于 75%。研究了不同浓度 Ce: LuAG 陶瓷在 454 nm 蓝光 LED 激发下的吸收和发射特性,获得了可调的相关色温(5 653 ~ 7 433 K)。所制备的 Ce: LuAG 陶瓷具有优异的热性能和发光性能,在 225 °C 下的 PL 强度较室温仅下降 7%, 0.1% Ce: LuAG 陶瓷在蓝光 LED 激发下的发光效率达到 179 lm/W。进一步研究了不同厚度 Ce: LuAG 陶瓷的发光饱和性能,1 mm 厚的 0.1% Ce: LuAG 陶瓷在功率密度为 24.6 W/mm² 的蓝光 LD 激发下获得了 3 646 lm 的高光通量,同时没有出现发光饱和现象。研究结果表明,Ce: LuAG 透明陶瓷具有高发光效率和热稳定性,适用于大功率固态照明。

关键词: 发光饱和; Ce: LuAG 陶瓷; 颜色转换器; 高亮度

1 Introduction

In recent years, with the continuous development of InGaN-based blue light-emitting diode (LED) and laser diode (LD), solid-state lighting (SSL) has attracted worldwide attentions in the lighting market for its great prospects^[1]. It replaces the traditional incandescent lighting source due to its advantages such as high integration, high energy efficiency, long lifetime, and environmental friendliness. The most mature commercial structure for SSL is the phosphor-converted white light-emitting diodes (pc-WLEDs). However, LEDs are limited by the well-known efficiency droop problem of the conversion efficiency of the LED chip dropping sharply under high input current. In contrast, the external quantum efficiency of laser diodes (LDs) increases linearly with the operating current, and the combination of color converter can achieve high-efficiency white light output^[2], which also makes laser diodes attractive as excitation sources for high-brightness white-light emission. As a result, SSL has broad application prospects in backlight display, car headlights, projection, and long-distance lighting.

The color converters are required to withstand the heavy thermal load and high-power density radiation from LEDs and LDs^[3]. Therefore, they should have high thermal conductivity for heat dissipation and low thermal quenching under long-term irradiation^[4]. However, the general strategy for producing phosphor-converted white light is to combine blue InGaN-GaN LEDs or LDs with Ce: YAG phosphor powders dispersed in organic silicone (PiS) at present^[5-6]. Due to the low thermal conductivity (0.1 – 0.4 W/(m · K)) and poor heat resistance of sili-

cone resin, PiS cannot withstand the excitation of high-power LDs/LEDs^[7-10]. To solve this problem, phosphor in glass (PiG)^[11-16] and phosphor ceramics^[17-20] are widely studied. However, PiG shows weak absorption, low heat resistance, and a luminescence saturation occurring at 1 W/mm²^[21], which is not suitable as high-power density LD-pumped phosphor. Phosphor ceramics are the most promising color converters due to their high heat resistance and high thermal conductivity. Ce: YAG based yellow emitting transparent ceramics have been widely studied currently^[22-24]. In contrast, Ce: LuAG has excellent thermal quenching performance^[25], high quantum efficiency^[26], and high luminescence efficiency. In addition, Ce: LuAG has a higher luminous saturation threshold under blue LD excitation. Therefore, Ce: LuAG color converters are well suited for high brightness SSL.

In particular, the ceramic thickness and the Ce³⁺ concentration are considered to significantly affect the optical properties of the white LED/LD^[27-29]. Thus, for high brightness SSL applications, it is necessary to carefully select the appropriate Ce³⁺ doping concentration and thickness of ceramic converters to achieve the high luminous flux and conversion efficiency at high excitation power. Moreover, the luminescence saturation under high power density excitation is an important performance index. Xu *et al.* reported that Ce: LuAG translucent ceramics showed increasing luminous flux (238 – 472 lm) with increasing laser driving power^[30]. Xu *et al.* reported Ce: LuAG phosphor ceramics with a high luminous flux of 3 967.3 lm at a super-high power density of 49 W/mm²^[31]. Ding *et al.* reported that the luminous efficacy of Ce: LuAG ceramic

was promoted to 216.9 lm/W, and the luminescence saturation was not observed at a laser power density of 19.75 W/mm²[32]. However, the influence of Ce:LuAG ceramics thickness on the luminescence saturation properties is rarely studied. Also, the effect of doping concentration on the luminescence performance of Ce:LuAG needs to be discussed in detail.

In this work, a series of Ce:LuAG transparent phosphor ceramics with different Ce³⁺ concentrations and different thicknesses were prepared *via* the solid-state reactive sintering method under vacuum. The XRD patterns, surface morphologies, in-line transmittance, absorption spectra, temperature-dependent photoluminescence (PL) and photoluminescence excitation (PLE) spectra of the obtained ceramics were systematically investigated. Besides, the luminescence properties such as luminous flux, color coordinates, CRI and CCT after combining the Ce:LuAG ceramics with a 454 nm blue LED were measured. The luminescence saturation performance of Ce:LuAG ceramics with distinct thickness under high power density laser driving was also evaluated.

2 Experiment

Ceramic samples with the chemical formula (Ce_xLu_{1-x})₃Al₅O₁₂ ($x = 0.0005, 0.001, 0.002, 0.003, 0.004$) were prepared by solid-state reaction at high temperature. High-purity powders of Lu₂O₃ (99.999%, Jining Zhongkai New Materials Co., Ltd, China), α -Al₂O₃ (99.99%, Yangzhou Zhongtianli Materchem Co., Ltd, China) and CeO₂ (99.99%, Fujian Changting Golden Dragon Rare-Earth Co., Ltd, China) were used as raw materials. The powders were ball milled for 12 h in ethanol, with 0.5% TEOS (>99.999%, Alfa Aesar, Tianjin, China) as sintering aids. Then the ethanol slurries were dried in oven at 70 °C for 2 h and sieved through a 200-mesh screen. The powder mixture was calcined in air at 600 °C for 4 h to remove the residual organics. Then, the calcined powders were uniaxially pressed at 40 MPa and cold isostatically pressed at 250 MPa into 20 mm disks to obtain green bodies. In order to obtain ceramics with different

Ce³⁺ concentration with similar optical quality, the green compacts with the designed composition of 0.2%, 0.3%, 0.4% Ce:LuAG were sintered at 1750 °C and the green bodies with designed composition of 0.05%, 0.1% Ce:LuAG were sintered at 1800 °C for 20 h under the vacuum of 5×10^{-3} Pa to prepare transparent Ce:LuAG ceramics.

After annealing at 1450 °C for 10 h in air, all the ceramic samples were double-surface polished for characterization and device packing.

The in-line transmittance curves and the absorption spectra were measured using a UV/VIS/NIR spectrophotometer (Cary 5000, Varian Medical System Inc. Palo Alto, USA). Microstructures of the obtained ceramics were observed by a field emission scanning electron microscope (FESEM, SU-8220, Hitachi, Japan). And average grain sizes of the sintered samples were calculated by the linear intercept method from the SEM images of the thermally etched ceramic surfaces. The phase information of the ceramics was characterized by X-ray diffraction (XRD, D8 Advance, Bruker, Germany) with nickel-filtered Cu K α radiation ($\lambda = 0.154056$ nm) in the 2θ range of 10°–80°. The temperature-dependent photoluminescence (PL) and photoluminescence excitation (PLE) spectra were tested using a fluorescence spectrophotometer (F-4600, Hitachi, Japan) equipped with a xenon lamp as the excitation source in the temperature ranges from 25 °C to 225 °C with a step size of 50 °C. These transparent ceramics were packaged with commercial 454 nm blue chips into LED chip-on board (COB) modules. The related room-temperature CCT, LE, CIE color coordinate and electroluminescent properties were measured using a high accuracy array spectroradiometer (HASS-2000, Hangzhou, China), with programmable LED test power supply (LED 300E, Hangzhou, China). The luminous flux of the phosphor ceramics with increasing incident laser power density was measured in a transmissive configuration by using a home-made system which consists of an integrating sphere (30 cm indiameter, Labsphere Inc., USA), a CCD spectrometer (F-4600, Japan Electronics Co., Ltd, Japan), and a high power light source

with a 450 nm blue laser (LSR-PS-FA, Lasever, China) and an incident power controller. The laser spot area is adjusted to 0.50 mm² by a lens system.

3 Results and Discussion

Fig. 1 shows the FESEM morphologies of the raw powder and the powder mixture after ball milling. There are severely agglomerated large particles in α -Al₂O₃ and Lu₂O₃ powders, and they are not sufficiently broken by the ball milling process.

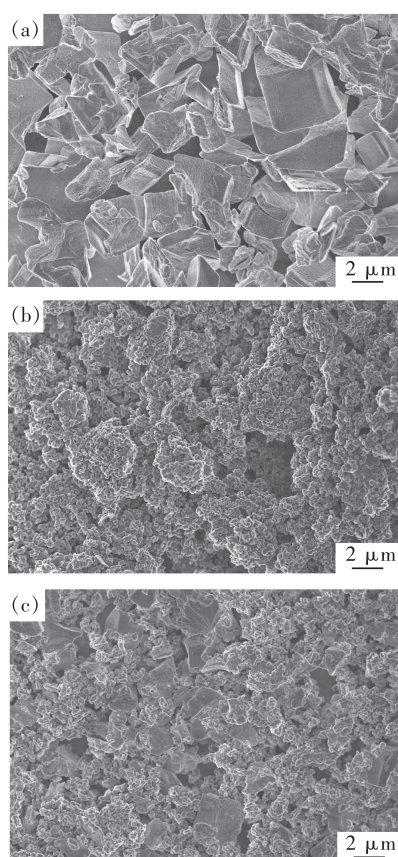


Fig. 1 FESEM morphologies of the starting powders. (a) Lu₂O₃. (b) α -Al₂O₃. (c) Powder mixture after ball milling.

Fig. 2 shows the photograph of transparent Ce: LuAG phosphor ceramics with different Ce³⁺ concentrations. The size of these ceramics is 15 mm in diameter and 1 mm in thickness. The characters on the paper can be clearly seen through these ceramic samples, indicating that the ceramics have good optical quality. Besides, the color of ceramics gradually changes from yellow-green to yellow with increasing Ce³⁺ concentration. It can be seen that there are

opaque areas in the 0.05%, 0.1%, 0.2% Ce: LuAG ceramics. In this work, CeO₂ plays the roles of not only a dopant but also a sintering aid in the fabrication of Ce: LuAG ceramics. When the doping concentration of Ce: LuAG ceramics is low, the driving force of densification is relatively weak. At the same time, due to the uneven dispersion of CeO₂ in the ball milled powder mixture, it is easy to cause the difference of local microstructure in Ce: LuAG ceramics, which eventually leads to the phenomenon of local opacity.

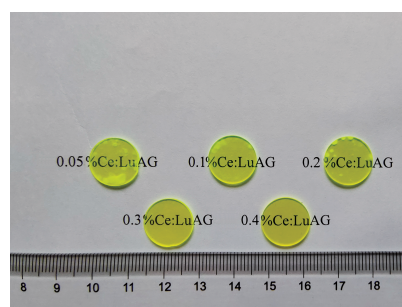


Fig. 2 Photograph of transparent Ce: LuAG ceramics with the thickness of 1.0 mm

The XRD patterns of Ce: LuAG transparent ceramics with various Ce³⁺ concentrations are showed in Fig. 3 (a). It can be seen that all the diffraction peaks of the ceramic samples perfectly match with the standard LuAG (PDF#73-1368), and no secondary phase is detected. Fig. 3 (b) shows the XRD patterns with expanded view of the 2 θ diffraction peaks between 33° and 34°. It can be seen clearly that the diffraction peaks shift towards to lower angle with the increase of Ce³⁺ concentration due to lattice expansion. The extended lattice can be explained by

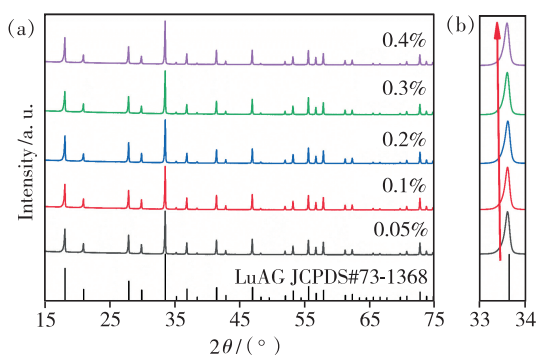


Fig. 3 (a) XRD patterns of Ce: LuAG ceramics with different Ce³⁺ doping concentrations. (b) Expanded view of the 2 θ diffraction peaks between 33° and 34°.

the fact that the ionic radius of Ce^{3+} ($r = 0.114$ nm, CN = 8) is bigger than that of Lu^{3+} ($r = 0.097$ nm, CN = 8), as shown in Tab. 1.

Tab. 1 Calculated cell parameters of Ce: LuAG with different Ce^{3+} doping concentrations

Ce concentration/%	Calculated cell parameter/nm
0.05	1.191 256
0.1	1.191 312
0.2	1.191 348
0.3	1.191 399
0.4	1.191 468
LuAG standard cell parameter	1.190 6

Fig. 4 shows the in-line transmittance curves and the absorption spectra of Ce: LuAG ceramics with various Ce^{3+} concentrations. It can be noted that the in-line transmittance of the ceramics with a thickness of 1.0 mm is more than 75% at 500–800 nm, which indicates that there is some light scattering caused by pores in the ceramics. Moreover, micro-sized pores inside the ceramics can improve the light extraction efficiency^[33]. Fig. 4(a) shows the broad absorption bands centered at 345 nm and 445 nm, corresponding to the $4f-5d_2$ and $4f-5d_1$ transitions

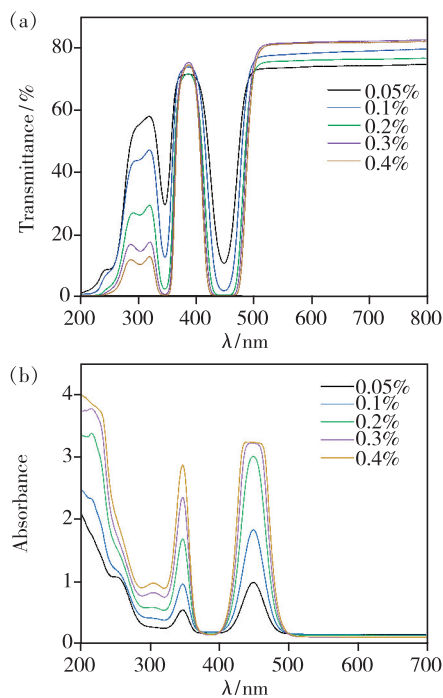


Fig. 4 In-line transmittance (a) and absorption spectra (b) of Ce: LuAG ceramics with various Ce^{3+} contents

of Ce^{3+} , respectively, indicating that the ceramics can be effectively excited by ultraviolet or blue light, which is better visually presented in the absorption spectra (Fig. 4(b)). The absorption peak intensity was enhanced with the increase of Ce content. An absorption saturation was found at 445 nm in 0.3% and 0.4% Ce: LuAG ceramics, which is an instrumental artifact due to perturbing effect of Ce^{3+} luminescence^[34]. The intensity of the absorption band around 300 nm increases linearly with the increase of Ce doping concentration, which may correspond to the f-f transitions of Gd^{3+} ^[35], while Gd^{3+} may be derived from CeO_2 raw material.

The microstructures of thermally-etched Ce: LuAG transparent ceramics with different Ce^{3+} contents are displayed in Fig. 5. Average grain sizes of Ce: LuAG ceramics with different Ce^{3+} contents (0.05%, 0.1%, 0.2%, 0.3%, 0.4%) are measured to be 131.5, 111.7, 58.3, 59.3, 58.5 μm , respectively. It can be seen from Fig. 5(a)–(e) that the bulges appear at the trigeminal grain boundaries in the Ce: LuAG ceramics. EDS analysis in Fig. 5(f) shows that the element content of the protruding part at the trigeminal grain boundary is basically in line with the $\text{Lu}_3\text{Al}_5\text{O}_{12}$ stoichiometric ratio, which may be caused by different surface heights resulting in different contrasts under FESEM, showing brighter white spots. Moreover, a small number of intra-granular pores are found in Fig. 5(a) and 5(b), which are attributed to the rapid growth of grains caused by the high sintering temperature of 1 800 $^\circ\text{C}$.

Fig. 6(a) presents the room-temperature excitation and emission spectra of transparent Ce: LuAG ceramics. The broad green-yellow emission bands from 475 nm to 700 nm are ascribed to the electron transitions from the lowest crystal-field splitting component of the $5d_1$ excited levels (2D) to the $4f$ ground state of Ce^{3+} ($^2F_{5/2}$, $^2F_{7/2}$). The emission intensity of Ce: LuAG ceramics increases firstly when the Ce^{3+} doping concentration increases from 0.05% to 0.2%, and then decreases with further increased Ce^{3+} concentration because of the concentration quenching effect^[36]. It can be observed that the

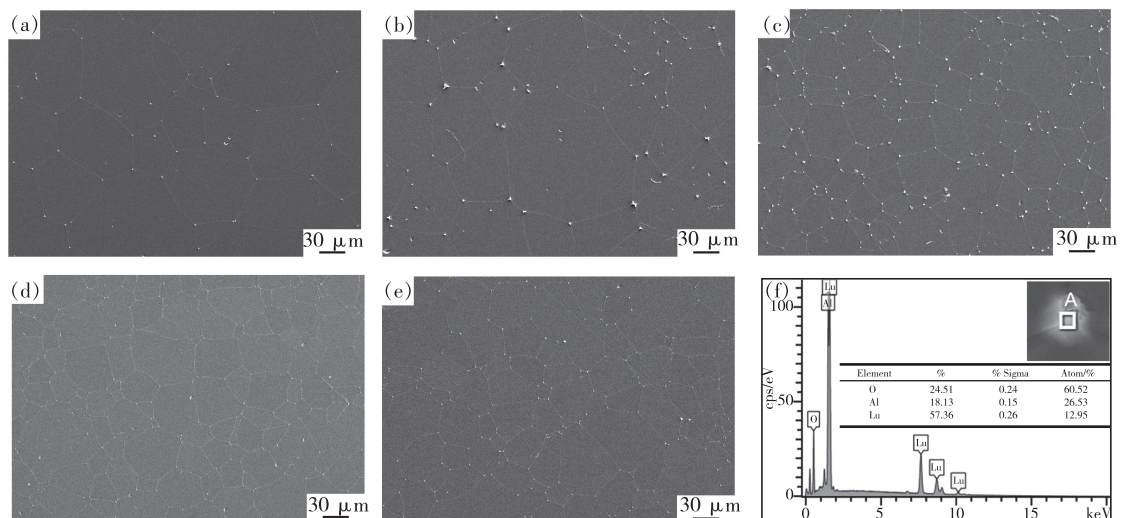


Fig. 5 FESEM photographs of double polished and thermally etched surfaces of Ce: LuAG transparent ceramics with 0.05% (a), 0.1% (b), 0.2% (c), 0.3% (d) and 0.4% (e) Ce^{3+} doping concentrations. (f) EDS analysis of the bulges at the trigeminal grain boundaries.

emission peak shifts from 507 nm for 0.05% Ce: LuAG to 515 nm for 0.4% Ce: LuAG. This is mainly due to the enhanced reabsorption of the short wavelength side of the Ce^{3+} emission and energy transfer between neighboring Ce^{3+} ions as the Ce^{3+} concentration increases^[37].

Temperature stability of Ce: LuAG ceramics was evaluated to verify whether it is suitable for SSL applications. Fig. 6 (b) shows the temperature-dependent PL spectra of 0.2% Ce: LuAG ceramics. As the temperature increases from 25 °C to 225 °C, the PL intensity decreases monotonically. From the integrated intensity and normalized intensity shown in Fig. 6(c), it can be seen that the relative PL intensity at 225 °C is only reduced by 7% compared to the room temperature PL intensity. As the temperature increases, a significant thermal red shift is caused by thermal excitation due to the stiff structure of Ce: LuAG^[38].

The luminescence properties of Ce: LuAG ceramics (1.0 mm thick) with different Ce^{3+} concentrations under excitation of 454 nm blue light LED with 0.6 W pump power were further studied, as shown in Tab. 2. All the ceramic samples show high luminous efficacy (LE), and the LE of Ce: LuAG ceramics increases firstly and then decreases with further increasing Ce^{3+} concentration. 0.1% Ce: LuAG ceramic sample obtains the highest LE of 179 lm/W.

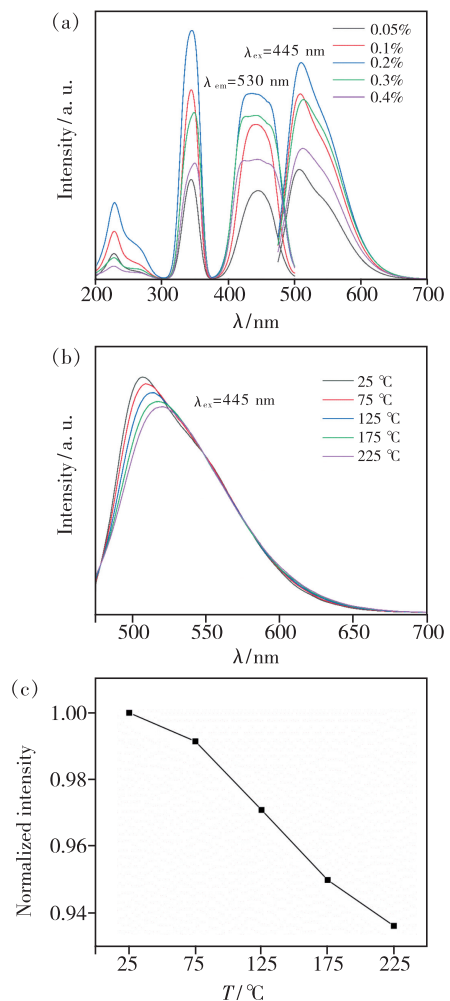


Fig. 6 (a) Room-temperature PL and PLE spectra of Ce: LuAG ceramics with various Ce^{3+} contents. (b) PL spectra of 0.2% Ce: LuAG ceramics measured at different temperatures. (c) Normalized PL intensity.

The decreased correlated color temperature (CCT) of ceramic samples (within the range of 7 433 – 5 653 K) indicates that the blue component in the spectra is decreasing. With the increase of Ce^{3+} concentra-

tion, the color coordinate also moves to the position with more green light components (change from (0.27, 0.43) to (0.32, 0.51)), indicating the decreasing blue/green ratio of the luminescence spectra.

Tab. 2 Luminescence properties of Ce:LuAG ceramics with various Ce^{3+} contents under 454 nm blue light excitation and 0.6 W pump power

Doping concentration/%	Luminous flux/lm	Luminous efficacy/(lm · W ⁻¹)	CRI	CCT/K	Color coordinates
0.05	100	171	50	7 433	(0.27, 0.43)
0.1	105	179	47	6 527	(0.29, 0.48)
0.2	101	173	46	6 049	(0.30, 0.50)
0.3	99	170	47	5 792	(0.31, 0.50)
0.4	96	165	47	5 653	(0.32, 0.51)

The electroluminescent (EL) spectra of Ce:LuAG ceramics are shown in Fig. 7. It reveals two peaks, one of which is centered at about 450 nm corresponding to the emission of the blue LED source, and the other wide band in the range of 475 nm to 750 nm is related to the emission of the ceramics. The blue emission intensity near 454 nm decreases with increasing Ce^{3+} concentration, which is attributed to the stronger absorption of the pumping blue light by increasing Ce^{3+} concentration. It is consistent with the change of CCT and color coordinates. However, similar or even lower luminous flux and luminous efficacy are obtained under different blue light absorptions, while yellow green light contributes to much more luminous flux than blue light, which indicates that Ce:LuAG ceramics with high doping concentration have a relatively low conversion efficiency (CE) (η_{CE}). η_{CE} is defined as the ratio of the converted green/yellow light to the absorbed blue light, which can be calculated using the following Eq. (1):

$$\eta_{\text{CE}} = \frac{P_2}{P_0 - P_1}, \quad (1)$$

where P_0 is the power of the incident blue LED, P_1 , P_2 are the 400 – 480 nm and 480 – 800 nm integral intensity corresponding to the EL spectra, respectively.

The conversion efficiencies of 0.05%, 0.1%, 0.2%, 0.3% and 0.4% Ce:LuAG ceramics are calculated to be 38.2%, 38.0%, 36.4%, 34.4%, and 33.8%, respectively. This is because that the

increase of Ce^{3+} concentration leads to more heat generation, and then the quantum efficiency of ceramics declines^[31]. So when the concentration of Ce^{3+} exceeds 0.1%, the luminous efficacy does not increase linearly with increasing Ce^{3+} concentration and even decreases slightly.

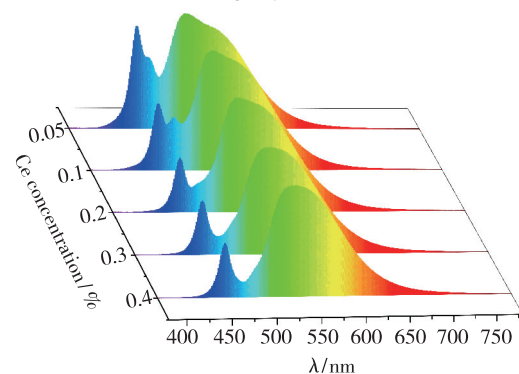


Fig. 7 Spectral performance of Ce:LuAG transparent ceramics with various Ce^{3+} contents under 454 nm blue light excitation and 0.6 W pump power with the thickness of 1.0 mm

Fig. 8(a) demonstrates the luminous illumination of white LED package using the 0.1% Ce:LuAG ceramics under blue light excitation with different incident pump powers ranging from 0.6 W to 3.6 W. With incident pump power increasing, the EL-intensity of the 0.1% Ce:LuAG ceramics increases without luminescence saturation. The luminous flux increases linearly and reaches 467 lm at 3.6 W, while the luminous efficacy of 0.1% Ce:LuAG ceramics decreases from 179 lm/W to 127 lm/W (Fig. 8(b)). This phenomenon can be explained by the effect of thermal quenching. With the increase of

input pump power, more energy will be dissipated in the form of heat through the non-radiative process, indicating that the luminous flux is not proportional to the input pump power. Therefore, the luminous efficacy obtained by the ratio of luminous flux/input power declines^[39].

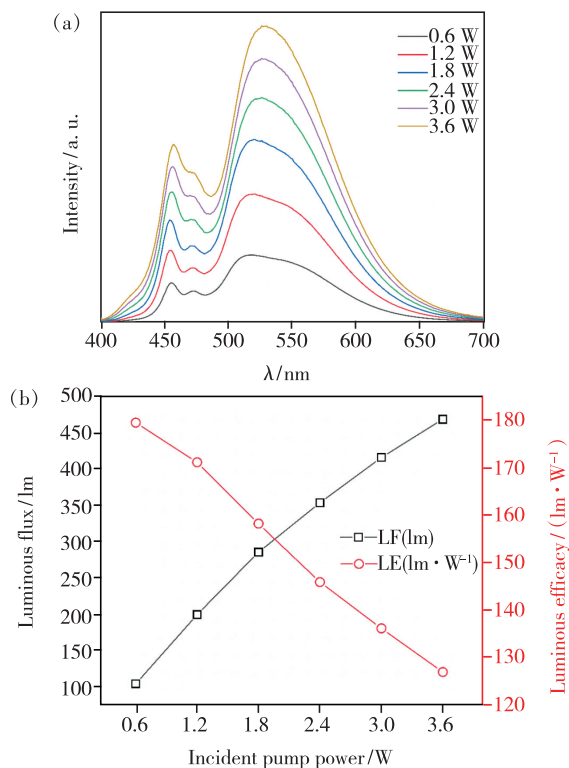


Fig. 8 (a) Driving-power-dependent electroluminescent (EL) spectra of the 0.1% Ce: LuAG ceramics. (b) Luminous flux and luminous efficacy as a function of incident pump power.

In order to verify the feasibility of color converter in high power laser lighting applications, we evaluated the lighting characteristics of phosphor ceramics, which were measured in the transmission mode and pumped by 450 nm blue LD. The relationship between luminous flux and pump power density of the 0.1% Ce: LuAG ceramics is shown in Fig. 9. The luminous flux of all the ceramics with different thicknesses linearly increases with the increase of

pump power, and there is no luminous saturation until the Ce: LuAG ceramics are broken under thermal shock without heat sink. As summarized in Tab. 3, for the thinner samples (0.3 mm and 0.6 mm), the increase of thickness can significantly improve the heat dissipation capacity, and the thicker ceramics have better mechanical properties, resulting in higher maximum power density (23.4 W/mm² for 0.6 mm thick sample and only 19.2 W/mm² for 0.3 mm thick sample). Moreover, the increasing thickness of the Ce: LuAG ceramics extends the light transmission path, and the blue light can be effectively absorbed by more emission centers, resulting in higher luminous flux (1 916 lm to 3 096 lm) and lower CCT (25 000 K to 12 897 K). Fig. 10 demonstrates the EL spectra of 0.1% Ce: LuAG ceramics with different thicknesses under 450 nm laser excitation with a laser power density of 19.2 W/mm². As the thickness of the ceramics increases, the intensity of blue light emission transmitted the ceramics decreases significantly, while the intensity of the converted yellow-green light emission increases. However, it also brings more heat generation, and there is a competitive effect between heat generation and heat dissipation when the thickness increases.

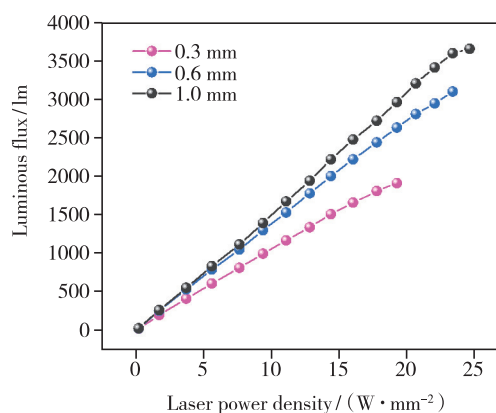


Fig. 9 Output luminous flux of 0.1% Ce: LuAG ceramics with different thicknesses as a function of incident laser power density

Tab. 3 Luminescence properties of 0.1% Ce: LuAG ceramics with different thicknesses under 450 nm blue LD excitation

Thickness/mm	Laser power density/(W · mm ⁻²)	Luminous flux/lm	CRI	CCT/K	Color coordinates
0.3	19.2	1 916	63	25 000	(0.21, 0.19)
0.6	23.4	3 096	65	12 897	(0.25, 0.30)
1.0	24.6	3 646	56	6 475	(0.30, 0.43)

For the further increasing thickness of ceramics (0.6 mm to 1.0 mm), the maximum power density and luminous flux no longer increase significantly. Enhanced blue light absorption results in lower CCT (6 475 K), and a high luminous flux of 3 646 lm is obtained at a laser power density of 24.6 W/mm².

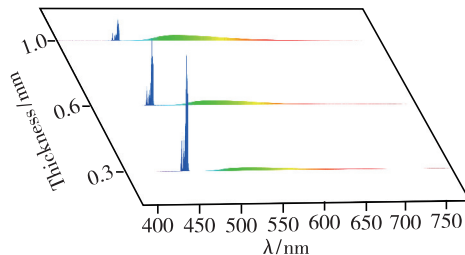


Fig. 10 EL spectra of 0.1% Ce:LuAG ceramics with different thicknesses under 450 nm laser excitation with a laser power density of 19.2 W/mm²

4 Conclusion

In summary, Ce:LuAG ceramics with various Ce³⁺ contents have been prepared by the solid-state reaction method. The 0.2% Ce:LuAG ceramic sample shows an excellent PL intensity and a low thermal quenching (7% drop at 225 °C). All the ceramics show an in-line transmittance of more than 75% at 800 nm with 1.0 mm thickness, which are suitable for SSL in the transmission mode. Absorption

and emission properties of Ce:LuAG ceramics with different doping concentrations excited by 454 nm blue LED were investigated. An adjustable CCT (5 653 – 7 433 K) was obtained. The 0.1% Ce:LuAG ceramics combined with blue LED exhibit an excellent luminous efficiency of 179 lm/W, and show an increasing emission intensity with increasing the input power (up to 3.6 W). The 0.1% Ce:LuAG ceramics with the thicknesses of 0.3, 0.6, 1.0 mm show increasing out luminous flux with the increase of input laser power density, and no luminescence saturation occurs at a laser power density of 19.2 – 24.6 W/mm². Under the excitation of blue LD in a transmission mode, the thicker Ce:LuAG ceramics have better heat dissipation capacity. A high flux of 3 646 lm was obtained at the laser power density of 24.6 W/mm² for the ceramic sample with the thickness of 1.0 mm. From these results, it is considered that Ce:LuAG transparent ceramics are quite prospective for a highly efficient and thermally robust green-yellow color converter for high-power SSL application.

Response Letter is available for this paper at: <http://cjl.lightpublishing.cn/thesisDetails#10.37188/CJL.20210116>.

References:

- [1] HAITZ R, TSAO J Y. Solid-state lighting: ‘the case’ 10 years after and future prospects [J]. *Phys. Status Solidi A*, 2011, 208(1):17-29.
- [2] WIERER JR J J, TSAO J Y, SIZOV D S. Comparison between blue lasers and light-emitting diodes for future solid-state lighting [J]. *Laser Photonics Rev.*, 2013, 7(6):963-993.
- [3] WANG J C, TANG X Y, ZHENG P, *et al.* Thermally self-managing YAG:Ce-Al₂O₃ color converters enabling high-brightness laser-driven solid state lighting in a transmissive configuration [J]. *J. Mater. Chem. C*, 2019, 7(13):3901-3908.
- [4] QIAO J W, ZHAO J, LIU Q L, *et al.* Recent advances in solid-state LED phosphors with thermally stable luminescence [J]. *J. Rare Earth.*, 2019, 37(6):565-572.
- [5] NAKAMURA S, SENOH M, MUKAI T. High-power InGaN/GaN double-heterostructure violet light emitting diodes [J]. *Appl. Phys. Lett.*, 1993, 62(19):2390-2392.
- [6] NAKAMURA S. High-power InGaN/AlGaN double-heterostructure blue-light-emitting diodes [C]. *Proceedings of 1994 IEEE International Electron Devices Meeting, San Francisco*, 1994:567-570.
- [7] 王兆武, 姬海鹏, 王飞翔, 等. 调控 Al₂O₃ 晶型控制 MgAl₂O₄:Mn⁴⁺ 荧光粉中 Mn 价态研究 [J]. *无机材料学报*, 2021, 36(5):513-520.
WANG Z W, JI H P, WANG F X, *et al.* Valence state control of manganese in MgAl₂O₄:Mn⁴⁺ phosphor by varying the Al₂O₃ crystal form [J]. *J. Inorg. Mater.*, 2021, 36(5):513-520. (in Chinese)

- [8] MING Z Q, ZHAO J, SWART H C, et al. Luminescence and energy transfer of color-tunable $\text{Lu}_2\text{MgAl}_4\text{SiO}_{12}:\text{Eu}^{2+}, \text{Ce}^{3+}, \text{Mn}^{2+}$ phosphors [J]. *J. Rare Earth.*, 2020, 38(5):506-513.
- [9] 孔丽, 乔露, 刘莹莹, 等. 白光 LED 用绿色荧光粉 $\text{Ba}_3(\text{PO}_4)_2:\text{Tb}^{3+}$ 的发光性能研究 [J]. *人工晶体学报*, 2019, 48(10):1869-1872.
- KONG L, QIAO L, LIU Y Y, et al. Study on the luminescent properties of green phosphor $\text{Ba}_3(\text{PO}_4)_2:\text{Tb}^{3+}$ for white LED [J]. *J. Synth. Cryst.*, 2019, 48(10):1869-1872. (in Chinese)
- [10] 董宇辉, 曾王玉, 韩博宁, 等. BN/CsPbX_3 复合纳米晶的制备及其白光 LED 应用 [J]. *无机材料学报*, 2019, 34(1):72-78.
- DONG Y H, ZENG S Y, HAN B N, et al. BN/CsPbX_3 composite nanocrystals: synthesis and applications in white LED [J]. *J. Inorg. Mater.*, 2019, 34(1):72-78. (in Chinese)
- [11] 郑飞, 茅云蔚, 杨波波, 等. 基于 YAG: Ce^{3+} 荧光粉复合 Eu^{3+} 掺杂荧光玻璃的激光照明器件 [J]. *发光学报*, 2019, 40(7):842-848.
- ZHENG F, MAO Y W, YANG B B, et al. Laser lighting device based on YAG: Ce^{3+} phosphor composite Eu^{3+} doped phosphor-in-glasses [J]. *Chin. J. Lumin.*, 2019, 40(7):842-848. (in Chinese)
- [12] ZHANG X J, SI S C, YU J B, et al. Improving the luminous efficacy and resistance to blue laser irradiation of phosphor-in-glass based solid state laser lighting through employing dual-functional sapphire plate [J]. *J. Mater. Chem. C*, 2019, 7(2):354-361.
- [13] PENG Y, MOU Y, SUN Q L, et al. Facile fabrication of heat-conducting phosphor-in-glass with dual-sapphire plates for laser-driven white lighting [J]. *J. Alloys Compd.*, 2019, 790:744-749.
- [14] CHEN H, LIN H, XU J, et al. Chromaticity-tunable phosphor-in-glass for long-lifetime high-power warm w-LEDs [J]. *J. Mater. Chem. C*, 2015, 3(31):8080-8089.
- [15] ZHONG J S, CHEN D Q, ZHOU Y, et al. Stable and chromaticity-tunable phosphor-in-glass inorganic color converter for high-power warm white light-emitting diode [J]. *J. Eur. Ceram. Soc.*, 2016, 36(7):1705-1713.
- [16] ZHANG R, LIN H, YU Y L, et al. A new-generation color converter for high-power white LED: transparent $\text{Ce}^{3+}:\text{YAG}$ phosphor-in-glass [J]. *Laser Photonics Rev.*, 2014, 8(1):158-164.
- [17] CAO Y F, HAN T, YANG J Y, et al. Tunable-spectrum Mn^{2+} doped garnet transparent ceramics for high-color rendering laser lighting [J]. *Int. J. Appl. Ceram. Technol.*, 2021, 18(3):716-723.
- [18] LING J R, ZHOU Y F, XU W T, et al. Red-emitting YAG: Ce, Mn transparent ceramics for warm WLEDs application [J]. *J. Adv. Ceram.*, 2020, 9(1):45-54.
- [19] JI E K, SONG Y H, BAK S H, et al. The design of a ceramic phosphor plate with functional materials for application in high power LEDs [J]. *J. Mater. Chem. C*, 2015, 3(48):12390-12393.
- [20] HUA H, FENG S W, OUYANG Z Y, et al. YAGG: Ce transparent ceramics with high luminous efficiency for solid-state lighting application [J]. *J. Adv. Ceram.*, 2019, 8(3):389-398.
- [21] ZHU Q Q, WANG X J, WANG L, et al. β -Sialon: Eu phosphor-in-glass: a robust green color converter for high power blue laser lighting [J]. *J. Mater. Chem. C*, 2015, 3(41):10761-10766.
- [22] ZHENG P, LI S X, WEI R, et al. Unique design strategy for laser-driven color converters enabling superhigh-luminance and high-directionality white light [J]. *Laser Photonics Rev.*, 2019, 13(10):1900147-1-10.
- [23] SONG Y H, JI E K, JEONG B W, et al. High power laser-driven ceramic phosphor plate for outstanding efficient white light conversion in application of automotive lighting [J]. *Sci. Rep.*, 2016, 6(1):31206-1-7.
- [24] YAO Q, HU P, SUN P, et al. YAG: Ce^{3+} transparent ceramic phosphors brighten the next-generation laser-driven lighting [J]. *Adv. Mater.*, 2020, 32(19):1907888-1-7.
- [25] MCKITTRICK J, SHEA-ROHWER L E. Review: down conversion materials for solid-state lighting [J]. *J. Am. Ceram. Soc.*, 2014, 97(5):1327-1352.
- [26] ZHANG Q, ZHENG R L, DING J Y, et al. High lumen density of Al_2O_3 -LuAG: Ce composite ceramic for high-brightness display [J]. *J. Am. Ceram. Soc.*, 2021, 104(7):3260-3268.
- [27] LIU G H, ZHOU Z Z, SHI Y, et al. Ce: YAG transparent ceramics for applications of high power LEDs: thickness effects and high temperature performance [J]. *Mater. Lett.*, 2015, 139:480-482.
- [28] WAETZIG K, KUNZER M, KINSKI I. Influence of sample thickness and concentration of Ce dopant on the optical properties of

- YAG: Ce ceramic phosphors for white LEDs [J]. *J. Mater. Res.*, 2014, 29(19):2318-2324.
- [29] HU S, LU C H, ZHOU G H, *et al.* Transparent YAG: Ce ceramics for WLEDs with high CRI: Ce³⁺ concentration and sample thickness effects [J]. *Ceram. Int.*, 2016, 42(6):6935-6941.
- [30] XU J, WANG J, GONG Y X, *et al.* Investigation of an LuAG: Ce translucent ceramic synthesized *via* spark plasma sintering: towards a facile synthetic route, robust thermal performance, and high-power solid state laser lighting [J]. *J. Eur. Ceram. Soc.*, 2018, 38(1):343-347.
- [31] XU Y R, LI S X, ZHENG P, *et al.* A search for extra-high brightness laser-driven color converters by investigating thermal-induced luminance saturation [J]. *J. Mater. Chem. C*, 2019, 7(37):11449-11456.
- [32] DING H, LIU Z H, HU P, *et al.* High efficiency green-emitting LuAG: Ce ceramic phosphors for laser diode lighting [J]. *Adv. Opt. Mater.*, 2021, 9(8):2002141.
- [33] ZHANG Y L, HU S, WANG Z J, *et al.* Pore-existing Lu₃Al₅O₁₂: Ce ceramic phosphor: an efficient green color converter for laser light source [J]. *J. Lumin.*, 2018, 197:331-334.
- [34] CHEN X P, HU Z W, CAO M Q, *et al.* Influence of cerium doping concentration on the optical properties of Ce, Mg: LuAG scintillation ceramics [J]. *J. Eur. Ceram. Soc.*, 2018, 38(9):3246-3254.
- [35] BARTOSIEWICZ K, BABIN V, KAMADA K, *et al.* Effects of Gd/Lu ratio on the luminescence properties and garnet phase stability of Ce³⁺ activated Gd_xLu_{3-x}Al₅O₁₂ single crystals [J]. *Opt. Mater.*, 2018, 80:98-105.
- [36] LIU Q, YUAN Y, LI J, *et al.* Preparation and properties of transparent Eu: YAG fluorescent ceramics with different doping concentrations [J]. *Ceram. Int.*, 2014, 40(6):8539-8545.
- [37] XIA Z G, MEIJERINK A. Ce³⁺-doped garnet phosphors: composition modification, luminescence properties and applications [J]. *Chem. Soc. Rev.*, 2017, 46(1):275-299.
- [38] CHIANG C C, TSAI M S, HON M H. Luminescent properties of cerium-activated garnet series phosphor: structure and temperature effects [J]. *J. Electrochem. Soc.*, 2008, 155(6):B517-B520.
- [39] LIU X, ZHOU H Y, HU Z W, *et al.* Transparent Ce: GdYAG ceramic color converters for high-brightness white LEDs and LDs [J]. *Opt. Mater.*, 2019, 88:97-102.



刘强(1964-),男,江苏镇江人,博士,教授,硕士研究生导师,2005年于江苏大学获得博士学位,主要从事发光材料和透明陶瓷等方面的研究。

E-mail: lq88611338@163.com



李江(1977-),男,浙江绍兴人,博士,研究员,博士研究生导师,2007年于中国科学院上海硅酸盐研究所获得博士学位,主要从事光功能透明陶瓷方面的研究。

E-mail: lijia@mail.sic.ac.cn